



Short Note

6-Bromo-*N*-(3-(difluoromethyl)phenyl)quinolin-4-amine

Christopher R. M. Asquith ^{1,2,*}  and Graham J. Tizzard ³ 

¹ Department of Pharmacology, University of North Carolina at Chapel Hill, Chapel Hill, NC 27599, USA

² Structural Genomics Consortium, UNC Eshelman School of Pharmacy, University of North Carolina at Chapel Hill, Chapel Hill, NC 27599, USA

³ UK National Crystallography Service, School of Chemistry, Highfield Campus, University of Southampton, Southampton SO17 1BJ, UK; Graham.Tizzard@soton.ac.uk

* Correspondence: chris.asquith@unc.edu; Tel.: +1-919-491-3177

Received: 9 October 2020; Accepted: 15 October 2020; Published: 20 October 2020



Abstract: A routine synthesis was performed to furnish the title compound which incorporates a versatile difluoromethyl group on the aniline substitution of a 4-anilinoquinoline kinase inhibitor motif. In addition, the small molecule crystal structure (of the HCl salt) was solved, which uncovered that the difluoromethyl group was disordered within the packing arrangement and also a 126.08(7)° out of plane character between the respective ring systems within the molecule. The compound was fully characterized with ¹H/¹³C-NMR and high-resolution mass spectra (HRMS), with the procedures described.

Keywords: 4-anilino-quin(az)olines; hinge binder; conformational flexibility; kinase inhibitor design

1. Introduction

The human kinome has shown impressive tractability, affording a number of high-profile clinical targets, which has led to the approval of more than 60 kinase inhibitors to date [1–3]. These drugs are for the most part multi-targeted tyrosine kinase inhibitors for the treatment of cancer [1–3]. There is an urgent need to develop highly selective compounds to open up the field into new indications beyond oncology [4]. However, this is not a straightforward task as all kinases bind a common substrate, adenosine triphosphate (ATP), which leads to a high degree of sequence homology across the kinome [5]. The 4-anilino-quin(az)oline scaffold shown is one of a number of hinge binders that have been shown to modulate kinome promiscuity, from broad spectrum such as GW559768X (1) to clinical narrow spectrum including lapatinib (2) and erlotinib and highly selective probes SGC-GAK-1 (3) (Figure 1) [6–13]. This kinome profile appears to be primarily driven by the electronics and substitution patterns of the pendant arms of the hinge binding scaffold [6–13].

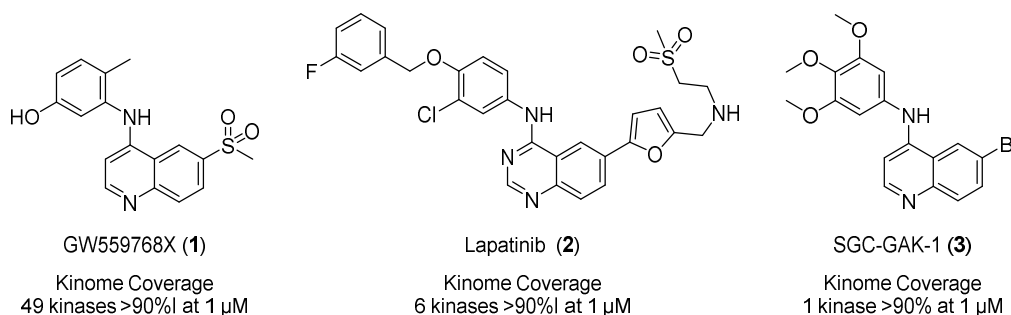


Figure 1. Previously reported 4-anilino-quin(az)olines (1–3) kinase inhibitors.

The difluoromethyl has shown a versatility in kinase inhibitor design, allowing the careful calibration of the compound properties [14–18]. These include potency profile, solubility and metabolic stability among others, several literature examples include PQR530 [19] and GDC-0077 [20,21] (Figure 2). We now describe incorporation of a difluoromethyl onto a known kinase active 6-bromoquinoline scaffold [6–10,22,23].

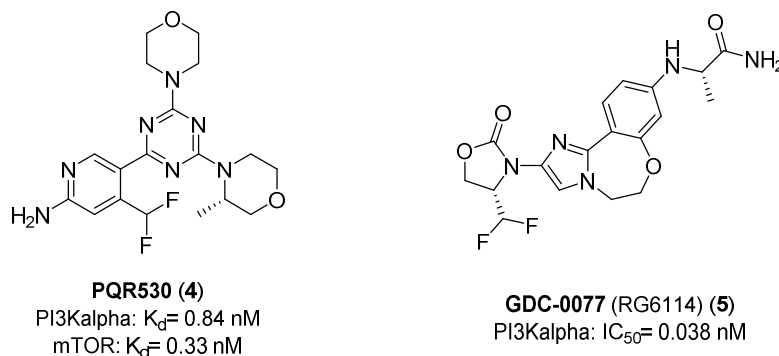
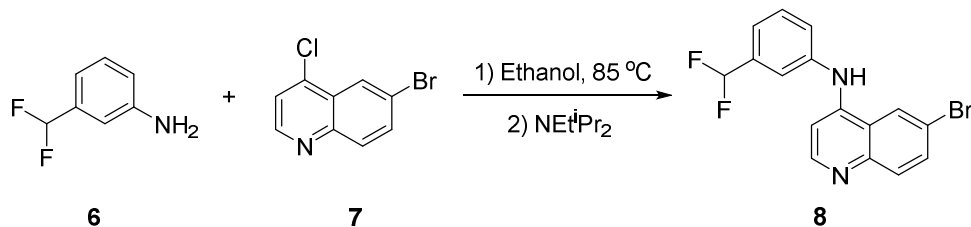


Figure 2. Examples of difluoromethyl use in kinase inhibitors (4,5).

2. Results

2.1. Synthesis of 8

The title compound was synthesized by a one-step protocol (Scheme 1) [22–29]. The corresponding 3-(difluoromethyl)aniline (**6**) and 6-bromo-4-chloroquinoline (**7**) were mixed and refluxed for 16 h followed by the addition of Hünig's base. The resulting mixture was purified to afford the title compound (**8**) in very good overall yield (83%) (see supporting information).



Scheme 1. Synthesis route to furnish 4-anilinoquinoline (**8**).

2.2. Crystal Structure of 8

A crystallographic analysis revealed **8** crystallized as the chloride salt with the difluoromethyl group disordered over two positions with approximate proportions of 70:30 throughout the crystal (Figure 3). The molecule comprises two planar moieties. The quinoline moiety, i.e., N1 and C1–C9 exhibits a root mean square (r.m.s.) deviation of 0.006 Å with the maximum deviation from the plane being -0.011 Å for C2. The r.m.s. deviation of the difluoromethylphenyl moiety, i.e., C10–C15, is 0.009 Å with C12 and C15 displaying the maximum deviation of -0.012 Å and -0.013 Å, respectively. The dihedral angle between the two aforementioned planes is $126.08(7)^\circ$. The C3–N2 bond distance of 1.342(3) Å is indicative of a double bond character in this bond consistent with conjugation in the quinoline moiety. All other bond distances and angles are within expected limits.

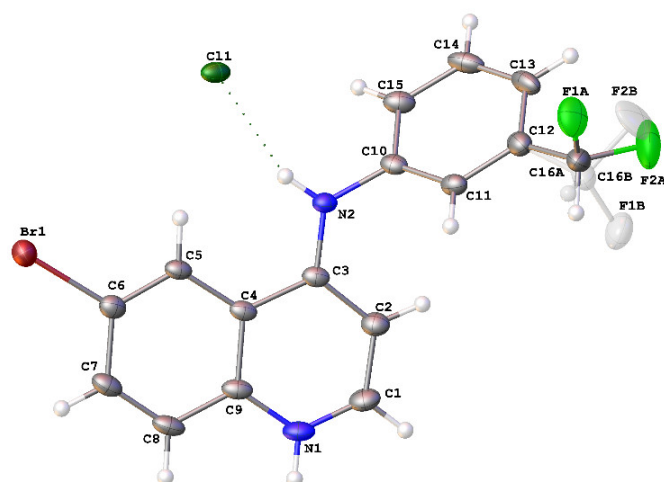


Figure 3. Molecular structure of $8\text{H}^+\text{Cl}^-$ showing atomic labelling and displacement ellipsoids at 50% probability level. The difluoromethyl minor disorder component is shown “ghosted”.

The chloride anion is integral to the solid-state structure. The structure comprises corrugated “tapes” of 8H^+ hydrogen bonded to Cl^- via the quinoline N-H^+ and aniline N-H , respectively ($\text{N-H}^+ \cdots \text{Cl}^- \cdots \text{H-N}$ (3.020(2) Å, 3.1113(19) Å)), parallel to the *b*-axis. These tapes form antiparallel stacks along the *a*-axis and close-pack along the *c*-axis to form the structure (Figure 4).

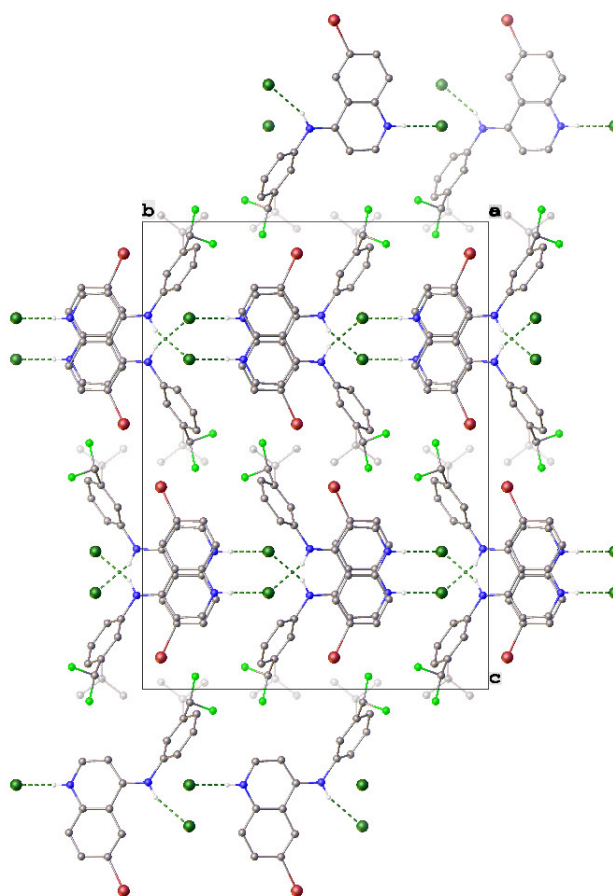


Figure 4. Unit cell contents of $8\text{H}^+\text{Cl}^-$ shown in projection down the *a*-axis. Hydrogen atoms except those involved in H-bonding are omitted for clarity. Hydrogen bonds are shown as dashed green lines. Minor disorder components are shown “ghosted”.

3. Discussion

We demonstrated a robust route to access the title compound (**8**) in excellent yield. This methodology lends itself to rapid library development as previously described [6–10,22–29]. The diversity of commercial and easy to synthetically access heterocycles and substitution patterns provide an endless wealth of possibilities and expandable chemical space to tune the 4-anilino-quin(az)oline scaffold properties for the discovery of new chemical tools and probes.

4. Material and Methods

4.1. Chemistry

All reactions were performed using flame-dried round-bottomed flasks or reaction vessels. Where appropriate, reactions were carried out under an inert atmosphere of nitrogen with dry solvents, unless otherwise stated. Yields refer to chromatographically and spectroscopically pure isolated yields. Reagents were purchased at the highest commercial quality and used without further purification. Reactions were monitored by thin-layer chromatography carried out on 0.25 mm E. Merck silica gel plates (60F-254) using ultraviolet light as visualizing agent. NMR spectra were recorded on a Varian Inova 400 (Varian, Palo Alto, CA, USA) and were calibrated using residual undeuterated solvent as an internal reference (CDCl₃: ¹H-NMR = 7.26, ¹³C-NMR = 77.16). The following abbreviations or combinations thereof were used to explain the multiplicities observed: s = singlet, d = doublet, t = triplet, q = quartet, m = multiplet, br = broad. Liquid chromatography (LC) and high-resolution mass spectra (HRMS) were recorded on a ThermoFisher hybrid LTQ FT (ICR 7T) (ThermoFisher, Waltham, MA, USA). The University of Southampton (Southampton, UK) small molecule x-ray facility collected and analyzed all X-ray diffraction data (Supplementary Materials).

6-Bromo-N-(3-(difluoromethyl)phenyl)quinolin-4-amine (**8**), 6-bromo-4-chloroquinoline (150 mg, 0.62 mmol, 1 eq) and 3-(difluoromethyl)aniline (97.3 mg, 0.68 mmol, 1.1 eq) were suspended in ethanol (10 mL) and refluxed for 18 h. This was followed by the addition of ¹Pr₂NEt (0.225 mL, 1.36 mmol, 2.2 eq.). The reaction mixture was concentrated in vacuo and extracted with ethyl acetate/saturated ammonium chloride. The title compound was then purified by flash chromatography using EtOAc: hexane followed by 1–5% methanol in EtOAc. The solvent was concentrated in vacuo and the product was obtained as a light beige solid (179 mg, 0.5134 mmol, 83%). MP 272–274 °C; ¹H-NMR (400 MHz, DMSO-*d*₆) δ 11.30 (s, 1H), 9.23 (d, *J* = 1.9 Hz, 1H), 8.56 (d, *J* = 6.9 Hz, 1H), 8.17 (dd, *J* = 9.0, 1.9 Hz, 1H), 8.12 (d, *J* = 9.0 Hz, 1H), 7.92–7.64 (m, 3H), 7.61 (dt, *J* = 6.4, 1.7 Hz, 1H), 7.14 (t, *J* = 55.7 Hz, 1H), 6.88 (d, *J* = 6.9 Hz, 1H). ¹³C-NMR (100 MHz, DMSO-*d*₆) δ 153.9, 143.2, 137.7, 137.4, 136.6, 135.8 (t, *J* = 22.5 Hz), 130.6, 127.6 (t, *J* = 2.1 Hz), 126.4, 124.5 (t, *J* = 6.0 Hz), 123.0–121.8 (2C, m), 120.0, 118.8, 114.3 (t, *J* = 236.7 Hz), 100.5. HRMS *m/z* [M + H]⁺ calcd for C₁₆H₁₂N₂BrF₂: 349.0152, found 349.0140, LC *t*_R = 3.78 min, >99% Purity.

4.2. Crystallography

Single colorless plate-shaped crystals of **8**H⁺Cl[−] were crystallized from EtOH/water and several drops of dioxane/HCL (4 M). A suitable crystal 0.16 × 0.10 × 0.02 mm³ was selected and mounted on a MITIGEN holder (MiTeGen, Ithaca, NY, USA) in perfluoroether oil on a Rigaku FRE+ equipped with VHF Varimax confocal mirrors and an AFC12 goniometer and HyPix 6000 detector. The crystal was kept at a steady *T* = 100(2) K during data collection. The structure was solved with the ShelXT [30] structure solution program using the using dual methods solution method and by using Olex2 [31] as the graphical interface. The model was refined with version 2018/3 of ShelXL [32] using full matrix least squares minimization on *F*² minimization. All non-hydrogen atoms were refined anisotropically. Hydrogen atom positions were calculated geometrically and refined using the riding model except for those bonded to N-atoms which were located in the difference map and refined with a riding model. The difluoromethyl group was disordered over two positions (ca. 70:30). Thermal restraints and 1,2 and 1,3 equal distance geometric restraints applied to all equivalent atom

pairs of disorder components. Equal distance geometric restraints were additionally applied to all C–F bonds.

Crystal Data for $C_{16}H_{12}N_2BrF_2Cl$ ($8H^+Cl^-$), $M_r = 385.64$, orthorhombic, $Pbca$ (No. 61), $a = 7.54250(10)$ Å, $b = 17.2573(4)$ Å, $c = 23.3121(7)$ Å, $a = b = c = 90^\circ$, $V = 3034.38(12)$ Å³, $T = 100(2)$ K, $Z = 8$, $Z' = 1$, $m(Mo K_\alpha) = 2.903$ mm⁻¹, 26,395 reflections measured, 5342 unique ($R_{int} = 0.0384$) which were used in all calculations. The final wR_2 was 0.0990 (all data) and R_1 was 0.0539 ($I \geq 2 s(I)$).

Supplementary Materials: The following are available online, ¹H and ¹³C NMR spectra and the crystallographic data for Compound $8H^+Cl^-$ in crystallographic information file (CIF) format. CCDC 2036373 also contains the supplementary crystallographic data for this paper. These data can be obtained free of charge via <http://www.ccdc.cam.ac.uk/conts/retrieving.html>.

Author Contributions: Conceptualization and writing the original draft preparation: C.R.M.A.; validation, resources, data curation and editing: C.R.M.A. and G.J.T. All authors have read and agreed to the published version of the manuscript.

Funding: The SGC is a registered charity (number 1097737) that receives funds from AbbVie, Bayer Pharma AG, Boehringer Ingelheim, Canada Foundation for Innovation, Eshelman Institute for Innovation, Genome Canada, Innovative Medicines Initiative (EU/EFPIA) (ULTRA-DD grant no. 115766), Janssen, Merck KGaA Darmstadt Germany, MSD, Novartis Pharma AG, Ontario Ministry of Economic Development and Innovation, Pfizer, São Paulo Research Foundation-FAPESP, Takeda, and Wellcome (106169/ZZ14/Z).

Acknowledgments: We thank the EPSRC UK National Crystallography Service at the University of Southampton for the collection of the crystallographic data. We also thank Brandie Ehrmann for LC–MS/HRMS support provided by the Mass Spectrometry Core Laboratory at the University of North Carolina at Chapel Hill.

Conflicts of Interest: The authors declare no conflict of interest.

References

1. Ferguson, F.M.; Gray, N.S. Kinase inhibitors: The road ahead. *Nat. Rev. Drug Discov.* **2018**, *17*, 353–377. [[CrossRef](#)] [[PubMed](#)]
2. Roskoski, R., Jr. Properties of FDA-approved small molecule protein kinase inhibitors. *Pharmacol. Res.* **2019**, *144*, 19–50. [[CrossRef](#)] [[PubMed](#)]
3. Roskoski, R., Jr. Properties of FDA-approved small molecule protein kinase inhibitors: A 2020 update. *Pharmacol. Res.* **2020**, *152*, 104609. [[CrossRef](#)] [[PubMed](#)]
4. Cohen, P.; Alessi, D.R. Kinase drug discovery—What’s next in the field? *ACS Chem. Biol.* **2013**, *8*, 96–104. [[CrossRef](#)]
5. Manning, G.; Whyte, D.B.; Martinez, R.; Hunter, T.; Sudarsanam, S. The protein kinase complement of the human genome. *Science* **2002**, *298*, 1912–1934. [[CrossRef](#)]
6. Asquith, C.R.M.; Laitinen, T.; Bennett, J.M.; Godoi, P.H.; East, M.P.; Tizzard, G.J.; Graves, L.M.; Johnson, G.L.; Dornsife, R.E.; Wells, C.I.; et al. Identification and Optimization of 4-Anilinoquinolines as Inhibitors of Cyclin G Associated Kinase. *ChemMedChem* **2018**, *13*, 48–66. [[CrossRef](#)]
7. Asquith, C.R.M.; Berger, B.T.; Wan, J.; Bennett, J.M.; Capuzzi, S.J.; Crona, D.J.; Drewry, D.H.; East, M.P.; Elkins, J.M.; Fedorov, O.; et al. SGC-GAK-1: A Chemical Probe for Cyclin G Associated Kinase (GAK). *J. Med. Chem.* **2019**, *62*, 2830–2836. [[CrossRef](#)]
8. Asquith, C.R.M.; Naegeli, N.; East, M.P.; Laitinen, T.; Havener, T.M.; Wells, C.I.; Johnson, G.L.; Drewry, D.H.; Zuercher, W.J.; Morris, D.C. Design of a cyclin G associated kinase (GAK)/epidermal growth factor receptor (EGFR) inhibitor set to interrogate the relationship of EGFR and GAK in chordoma. *J. Med. Chem.* **2019**, *62*, 4772–4778. [[CrossRef](#)]
9. Asquith, C.R.M.; Treiber, D.K.; Zuercher, W.J. Utilizing comprehensive and mini-kinome panels to optimize the selectivity of quinoline inhibitors for cyclin G associated kinase (GAK). *Bioorg. Med. Chem. Lett.* **2019**, *29*, 1727–1731. [[CrossRef](#)]
10. Asquith, C.R.M.; Bennett, J.M.; Su, L.; Laitinen, T.; Elkins, J.M.; Pickett, J.E.; Wells, C.I.; Li, Z.; Willson, T.M.; Zuercher, W.J. Development of SGC-GAK-1 as an orally active in vivo probe for cyclin G associated kinase through cytochrome P450 inhibition. *bioRxiv* **2019**, 629220. [[CrossRef](#)]

11. Drewry, D.H.; Wells, C.I.; Andrews, D.M.; Angell, R.; Al-Ali, H.; Axtman, A.D.; Capuzzi, S.J.; Elkins, J.M.; Ettmayer, P.; Frederiksen, M.; et al. Progress towards a public chemogenomic set for protein kinases and a call for contributions. *PLoS ONE* **2017**, *12*, e0181585. [[CrossRef](#)] [[PubMed](#)]
12. Fabian, M.A.; Biggs, W.H., III; Treiber, D.K.; Atteridge, C.E.; Azimioara, M.D.; Benedetti, M.G.; Carter, T.A.; Ciceri, P.; Edeen, P.T.; Floyd, M.; et al. A small molecule-kinase interaction map for clinical kinase inhibitors. *Nat. Biotechnol.* **2005**, *23*, 329–336. [[CrossRef](#)] [[PubMed](#)]
13. Karaman, M.W.; Herrgard, S.; Treiber, D.K.; Gallant, P.; Atteridge, C.E.; Campbell, B.T.; Chan, K.W.; Ciceri, P.; Davis, M.I.; Edeen, P.T.; et al. A quantitative analysis of kinase inhibitor selectivity. *Nat. Biotechnol.* **2008**, *26*, 127–132. [[CrossRef](#)] [[PubMed](#)]
14. Shah, P.; Westwell, A.D. The role of fluorine in medicinal chemistry. *J. Enzyme Inhib. Med. Chem.* **2007**, *22*, 527–540. [[CrossRef](#)]
15. Hagmann, W.K. The Many Roles for Fluorine in Medicinal Chemistry. *J. Med. Chem.* **2008**, *51*, 4359–4369. [[CrossRef](#)]
16. Swallow, S. Chapter Two-Fluorine in Medicinal Chemistry. *Prog. Med. Chem.* **2015**, *54*, 65–133. [[CrossRef](#)]
17. Wang, Y.; Callejo, R.; Slawin, A.M.Z.; O'Hagan, D. The difluoromethylene (CF₂) group in aliphatic chains: Synthesis and conformational preference of palmitic acids and nonadecane containing CF₂ groups Beilstein. *J. Org. Chem.* **2014**, *10*, 18–25. [[CrossRef](#)]
18. Corr, M.J.; Cormanich, R.A.; von Hahmann, C.N.; Bühl, M.; Cordes, D.B.; Slawin, A.M.Z.; O'Hagan, D. Fluorine in fragrances: Exploring the difluoromethylene (CF₂) group as a conformational constraint in macrocyclic musk lactones. *Org. Biomol. Chem.* **2016**, *14*, 211. [[CrossRef](#)]
19. Rageot, D.; Bohnacker, T.; Keles, E.; McPhail, J.A.; Hoffmann, R.M.; Melone, A.; Borsari, C.; Sriramaratnam, R.; Sele, A.M.; Beaufils, F.; et al. (S)-4-(Difluoromethyl)-5-(4-(3-methylmorpholino)-6-morpholino-1,3,5-triazin-2-yl)pyridin-2-amine (PQR530), a potent, orally bioavailable, and brain-penetrable dual inhibitor of class I PI3K and mTOR kinase. *J. Med. Chem.* **2019**, *62*, 6241–6261. [[CrossRef](#)]
20. Braun, M.-G.; Hanan, E.; Staben, S.T.; Heald, R.A.; MacLeod, C.; Elliott, R. Benzoxazepin Oxazolidinone Compounds and Methods of Use. U.S. Patent Application 20,170,210,733, 16 May 2017.
21. Han, C.; Kelly, S.M.; Cravillion, T.; Savage, S.J.; Nguyen, T.; Gosselin, F. Synthesis of PI3K inhibitor GDC-0077 via a stereocontrolled *N*-arylation of α -amino acids. *Tetrahedron* **2019**, *75*, 4351–4357. [[CrossRef](#)]
22. Asquith, C.R.M.; Tizzard, G.J.; Bennett, J.M.; Wells, C.I.; Elkins, J.M.; Willson, T.; Poso, A.; Laitinen, T. Targeting the water network in cyclin G associated kinase (GAK) with 4-anilino-quin(az)oline inhibitors. *ChemMedChem* **2020**, *15*, 1200–1215. [[CrossRef](#)]
23. Asquith, C.R.M.; Laitinen, T.; Bennett, J.M.; Wells, C.I.; Elkins, J.M.; Zuercher, W.J.; Tizzard, G.J.; Poso, A. Design and analysis of the 4-anilino-quin(az)oline kinase inhibition profiles of GAK/SLK/STK10 using quantitative structure activity relationships. *ChemMedChem* **2020**, *15*, 26–49. [[CrossRef](#)] [[PubMed](#)]
24. Saul, S.; Pu, S.; Zuercher, W.J.; Einav, S.; Asquith, C.R.M. Potent antiviral activity of novel multi-substituted 4-anilinoquin(az)olines. *Bioorg. Med. Chem. Lett.* **2020**, *30*, 127284. [[CrossRef](#)] [[PubMed](#)]
25. Asquith, C.R.M.; Laitinen, T.; Wells, C.I.; Tizzard, G.J.; Zuercher, W.J. New insights into 4-anilinoquinazolines as inhibitors of cardiac troponin I-interacting kinase (TNNi3K). *Molecules* **2020**, *25*, 1697. [[CrossRef](#)]
26. Asquith, C.R.M.; Tizzard, G.J. 6-Bromo-N-(2-methyl-2H-benzo[d][1,2,3]triazol-5-yl)quinolin-4-amine. *Molbank* **2019**, 2019, 1087. [[CrossRef](#)]
27. Carabajal, M.A.; Asquith, C.R.M.; Laitinen, T.; Tizzard, G.J.; Yim, L.; Rial, A.; Chabalgoity, J.; Zuercher, W.J.; Vescovi, E.G. Quinazoline-based anti-virulence compounds that selectively target Salmonella PhoP/PhoQ signal transduction system. *Antimicrob. Agents Chemother.* **2019**, *64*, e01744-19. [[CrossRef](#)] [[PubMed](#)]
28. Asquith, C.R.M.; Fleck, N.; Torrice, C.D.; Crona, D.J.; Grundner, C.; Zuercher, W.J. Anti-tubercular activity of novel 4-anilinoquinolines and 4-anilinoquinazolines. *Bioorg. Med. Chem. Lett.* **2019**, *18*, 2695–2699. [[CrossRef](#)] [[PubMed](#)]
29. Asquith, C.R.M.; Maffuid, K.A.; Laitinen, T.; Torrice, C.D.; Tizzard, G.J.; Crona, D.J.; Zuercher, W.J. Targeting an EGFR water network using novel 4-anilinoquin(az)olines inhibitors for chordoma. *ChemMedChem* **2019**. [[CrossRef](#)]
30. Sheldrick, G.M. ShelXT-Integrated space-group and crystal-structure determination. *Acta Cryst.* **2015**, *A71*, 3–8. [[CrossRef](#)]

31. Dolomanov, O.V.; Bourhis, L.J.; Gildea, R.J.; Howard, J.A.K.; Puschmann, H. Olex2: A complete structure solution, refinement and analysis program. *J. Appl. Cryst.* **2009**, *42*, 339–341. [[CrossRef](#)]
32. Sheldrick, G.M. Crystal structure refinement with ShelXL. *Acta Cryst.* **2015**, *C27*, 3–8. [[CrossRef](#)]

Publisher's Note: MDPI stays neutral with regard to jurisdictional claims in published maps and institutional affiliations.



© 2020 by the authors. Licensee MDPI, Basel, Switzerland. This article is an open access article distributed under the terms and conditions of the Creative Commons Attribution (CC BY) license (<http://creativecommons.org/licenses/by/4.0/>).